scientific reports

Check for updates

OPEN

Metabolic profiling unveils enhanced antibacterial synergy of polymyxin B and teixobactin against multi-drug resistant *Acinetobacter baumannii*

Maytham Hussein[1]✉, Zhisen Kang[1], Stephanie L. Neville[2], Rafah Allobawi[1], Varsha Thrombare[1], Augustine Jing Jie Koh[1,3], Jonathan Wilksch[2], Simon Crawford[4], Mudher Khudhur Mohammed[5], Christopher A. McDevitt[2], Mark Baker[6], Gauri G. Rao[7]✉, Jian Li[4]✉ & Tony Velkov[1]✉

This untargeted metabolomics study investigated the synergistic antibacterial activity of polymyxin B and Leu_{10}-teixobactin, a depsipeptide inhibitor of cell wall biosynthesis. Checkerboard microdilution assays revealed a significant synergy against polymyxin-susceptible and -resistant *A. baumannii*, excluding lipopolysaccharide-deficient variants. Time-kill assays confirmed bactericidal synergy, reducing bacterial burden by approximately 4-6-log_{10}CFU/mL. The combination (2xMIC polymyxin B and 0.5xMIC Leu_{10}-teixobactin) prevented bacterial regrowth after 24 h, indicating sustained efficacy against the emergence of resistant mutants. The analysis of *A. baumannii* ATCC™ 19606 metabolome demonstrated that the polymyxin B–Leu_{10}-teixobactin combination produced more pronounced perturbation compared to the individual antibiotics across all time points (1, 3 and 6 h). Pathway analysis revealed that lipid metabolism, cell envelope biogenesis, and cellular respiration were predominantly impacted by the combination, and to a lesser extent by polymyxin B monotherapy. Leu_{10}-teixobactin treatment alone had only a minor impact on the metabolome, primarily at the 6 h time point. Peptidoglycan assays confirmed the combination's concerted deleterious effects on bacterial cell envelope integrity. Electron microscopy further substantiated these findings, revealing pronounced cell envelope damage, membrane blebbing, and vacuole formation. These findings highlight the potential of the polymyxin B–Leu_{10}-teixobactin combination as an effective treatment in preventing resistance in *A. baumannii*.

Keywords Polymyxin B, Teixobactin, *A. baumannii*, Antimicrobial resistance, Metabolomics

Acinetobacter baumannii has evolved into a serious threat to global public health, causing high mortality rates, prolonged hospital admissions, and increased healthcare costs[1,2]. The overuse and misuse of antibiotics, even extending to the last line polymyxins, as well as the sparse anti-Gram-negative antibiotic pipeline are the main causes of this global calamity[3]. Worryingly, many nosocomial *A. baumannii* isolates have become extraordinarily resistant to almost all currently used antibiotics, including polymyxins[4]. The World Health Organization (WHO) has categorized *A. baumannii* as a critical priority pathogen in urgent need for the development of new

[1]Monash Biomedicine Discovery Institute, Department of Pharmacology, Monash University, Clayton, VIC 3800, Australia. [2]Department of Microbiology and Immunology, The Peter Doherty Institute for Infection and Immunity, The University of Melbourne, Parkville, VIC 3010, Australia. [3]Department of Biochemistry and Pharmacology, School of Biomedical Sciences, Faculty of Medicine, Dentistry and Health Sciences, The University of Melbourne, Parkville, VIC 3010, Australia. [4]Monash Biomedicine Discovery Institute, Department of Microbiology, Monash University, Clayton, VIC 3800, Australia. [5]Department of Pharmacy, Al-Manara college for medical sciences, Maysan, Iraq. [6]Discipline of Biological Sciences, Priority Research Centre in Reproductive Biology, Faculty of Science and IT, University of Newcastle, University Drive, Callaghan, NSW 2308, Australia. [7]Titus Family, Department of Clinical Pharmacy, University of Southern California, 1985 Zonal Avenue, Los Angeles, CA 90089-9121, USA. ✉email: maytham.hussein.old@monash.edu; gaurirao@usc.edu; jian.li@monash.edu; tony.velkov@monash.edu

antibiotics[5,6]. Given that the clinical pipeline for new anti-Gram-negative antibiotics is sparse, combinatorial approaches, wherein two or more antibiotics are used in combination to overcome their individual limitations, have emerged as an effective solution[7,8].

Polymyxins (polymyxin B and colistin) were discovered approximately 80 years ago but fell out of favor among clinicians during the 1970s[9]. This decline in usage was primarily attributed to nephro- and neurotoxicity; coupled with the introduction of better- tolerated antibiotic classes, namely the β-lactams[9,10]. In recent times, the emergence of difficult to treat multi-drug resistant (MDR) Gram-negative pathogens has spurred a renewed interest in polymyxins as antibiotics of last-resort[9]. However, reports of polymyxin resistance particularly in *A. baumannii*, have become widespread[11,12]. This misfortunate necessitates the development of new and effective strategies, such as combination therapies, that serve to extend polymyxin efficacy, ameliorate toxicity, and perturb the development of resistant mutants[13]. It is a widely understood that polymyxins exert their antibacterial action primarily by disrupting the bacterial outer membrane via direct interactions with lipopolysaccharide (LPS); however, the precise intricacies of this mechanism of action are still unfolding[14].

Teixobactin is an unique depsipeptide, that was first isolated through screening of unculturable soil bacteria, which led to the discovery of the producing organism namely *Eleftheria terrae*[15]. Native teixobactin contains four D-amino acids, N-Me-D-Phe1, D-Gln4, D-allo-Ile5 and D-Thr8, and the uncommon L-allo-enduracididine10 (L-allo-End) residue[15]. The synthesis of L-allo-End, a cyclic arginine analogue, poses a significant challenge as it is not commercially available[16]. In response, Leu_{10}-teixobactin was developed as a synthetic analogue, substituting the synthetically challenging enduracididine with commercially available hydrophobic residues, leucine and isoleucine[17]. Multiple studies have demonstrated that Leu_{10}-teixobactin exhibits equivalent antibacterial activities to native teixobactin[18–21]. The mode of action of teixobactin primarily involves inhibition of the bacterial cell wall synthesis. It synergistically targets two main intermediates, lipid I and lipid II, both of which serve as enzymatic substrates and precursors in the biosynthesis of the cell wall components, peptidoglycan and wall teichoic acid (WTA)[15,22]. By disrupting bacterial cell wall biosynthesis, teixobactin weakens cell wall structure, resulting in bactericidal effects through autolysis, a mechanism initially elucidated in Gram-positive bacteria[15,23].

Native teixobactin and Leu_{10}-teixobactin lack intrinsic activity against Gram-negative bacteria due to the highly impermeable Gram-negative outer membranes, that hinders their entry into the cell. Albeit, Leu_{10}-teixobactin has been shown to exhibit antibacterial activity against a mutant strain of *Escherichia. coli asmB1*, which has a defective outer membrane[15]. Furthermore, the hypothesis of outer membrane blockade is also supported by the acquired activity of teixobactin analogues when combined with sub-MIC levels of colistin against *P. aeruginosa* PAO1[26]. This suggests the potential for combining teixobactin with outer-membrane-acting antibiotics like polymyxins to combat other problematic Gram-negative bacteria such as *A. baumannii*[24].

The present study aimed to evaluate the metabolomic mechanisms underlying the antibacterial synergy of Leu_{10}-teixobactin in combination with polymyxin B against *A. baumannii*. Additionally, electron microscopy and peptidoglycan assay were utilized to further elucidate the mechanism of action. The results presented herein underlie the effective synergy and clinical potential of the polymyxin B-Leu_{10}-teixobactin combination for the treatment of MDR *A. baumannii* infections.

Results and discussions

Synergy testing of polymyxin B–Leu_{10}-teixobactin combinations (fractional inhibitory concentration index (FICI) calculation) against a panel of clinical *A. baumannii* isolates

The synergistic antibacterial activity of the polymyxin B and Leu_{10}-teixobactin combination was tested against four polymyxin-susceptible and eight polymyxin-resistant clinical isolates of *A. baumannii* (Supplementary Table S1). The results showed that the combination exhibited synergistic antibacterial effects against all tested strains, with the exception of two strains: namely *A. baumannii* FADDI-AB065 (lipopolysaccharide-deficient strain, polymyxin B MIC = 64 mg/L), indifference FICI = 2; and *A. baumannii* FADDI-AB151(polymyxin B MIC = 2 mg/L), additive FICI = 0.62. All strains were exposed to a final concentration of DMSO (0.01%, v/v), which did not inhibit their growth. The experiments were conducted in triplicate to ensure consistency and reliability of the results.

Static time-kill studies

A static time-kill assay was conducted to assess the effect of the combination on bacterial growth over time using strain *A. baumannii* ATCC™ 19606. The logarithmic phase bacterial culture (CFU/mL = 1×10^6) was exposed to varying concentrations of the antibiotics alone or in combination at different multiples of MICs (i.e., 0.5xMIC, 1xMIC, 2xMIC; Fig. 1).

The killing kinetics curves showed that polymyxin B monotherapy (0.5xMIC, 1xMIC, 2xMIC) initially decreased the bacterial burden by 2-5-fold over the 1–4 h period (log_{10}CFU/mL) compared to the untreated control. However, there was noticeable regrowth observed at 24 h, suggesting that *A. baumannii* ATCC™19606 developed resistance against polymyxin B[25]. On the other hand, Leu_{10}-teixobactin monotherapy (0.5xMIC) only caused a slight reduction in log_{10}CFU/mL (~ 1.5-fold) compared to the untreated control at 4 and 24 h (Fig. 1). According to CLSI guidelines for defining bactericidal synergy (≥ 2 log_{10} CFU/mL reduction *versus* the most active agent), it can be said that the polymyxin B-Leu_{10}-teixobactin combination produced a marked decline (≥ 2-fold decrease) in bacterial growth compared to polymyxin B monotherapy at early time points (i.e., 1 and 4 h)[26]. This effect was even more pronounced at 24 h, resulting in a 4-6-log_{10} CFU/mL decrease in bacterial load with the combination treatment compared to the tested monotherapy concentrations.

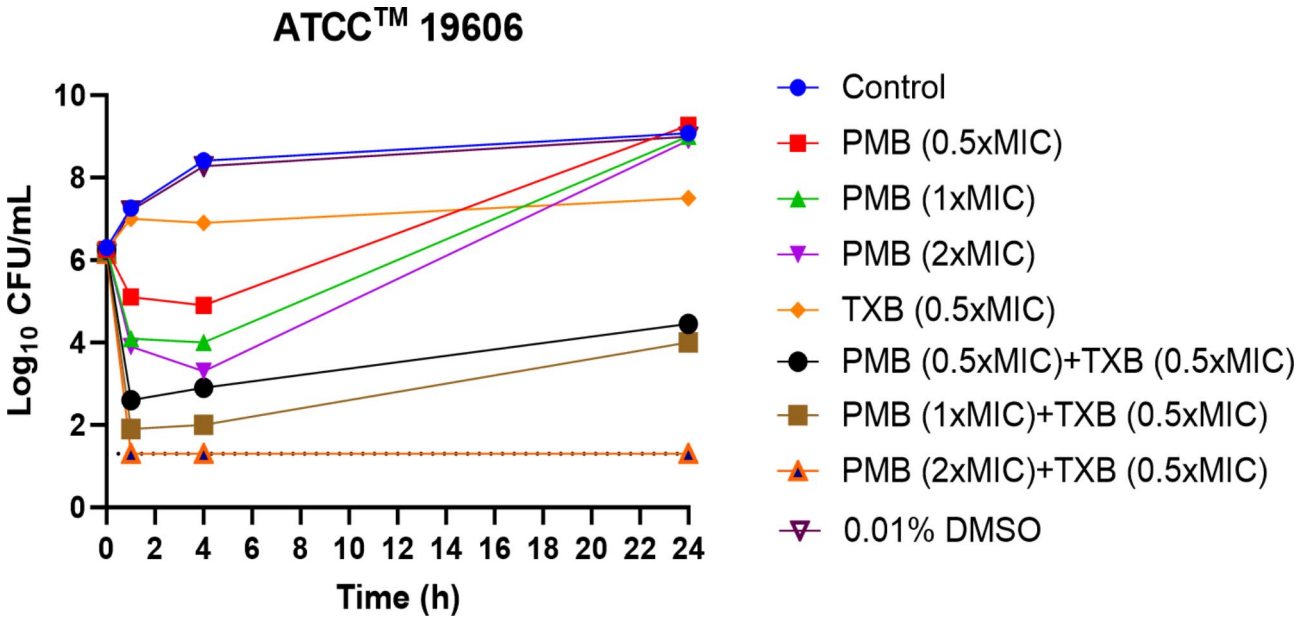

Fig. 1. Time-kill curve for polymyxin B and Leu_{10}-teixobactin monotherapies, and their combinations against*A. baumannii*ATCC™ 19606 (Polymyxin B MIC = 1 mg/L; Leu_{10}-teixobactin MIC = 8 mg/L) at 1, 3 and 6 h. Data are reported as mean values of three independent cultures, and the vertical bars represent the standard deviations. Error bars are too small to appear in the graphs. The grid line represents the lower detection limit for log_{10}CFU/mL at 1.3. PMB = Polymyxin B; TXB = Leu_{10}-teixobactin.

Metabolomics analysis of antibacterial synergy

Metabolomics data profiling and annotation identified 903 putative metabolites across all time points (1, 3 and 6 h) in response to all treatment conditions. These metabolites represent both those that were altered in response to treatment, and those that remained unchanged. The 903 metabolites can be further categorised as peptides ($n = 239$), amino acids ($n = 159$) and lipids ($n = 130$) formed the majority of metabolite classes, followed by carbohydrates ($n = 53$), nucleotides ($n = 42$), cofactors and vitamins ($n = 25$), secondary metabolites ($n = 11$), undefined metabolites ($n = 234$) and the least abundant class was metabolites involved in energy metabolism ($n = 10$; Supplementary Figure S1).

The significantly perturbed metabolites were identified using one-way analysis of variance (ANOVA) (log_2-fold change (FC) ≥ 0.58 or $\leq$ -0.58, corresponding to a metabolite level change of approximately 1.5-fold; FDR-adjusted p-value < 0.05). Principal component analysis (PCA) plots demonstrated a notable overlapping between the samples treated with the combination and those treated with polymyxin B monotherapy across all time points (1, 3, and 6 h), suggesting that the combination's antibacterial effect is likely driven by polymyxin B (Supplementary Figure S2A). In contrast, samples treated with Leu_{10}-teixobactin alone showed minimal distinction from the untreated control groups during the initial exposure periods (i.e., at 1 and 3 h), with a slight overlap observed at 6 h with the combination treatment. This suggests that Leu_{10}-teixobactin may contribute to the combination effect in a delayed time-dependent manner, which would be in line with its known action against cell wall biogenesis (Supplementary Figure S2A). Moreover, this finding aligns with the time-delayed antibacterial activity of native teixobactin against the Gram-positive strain *Staphylococcus aureus* NCTC8325 in the original *Nature* report[15]. The same pattern of differences between treated and untreated (control) groups was reflected in the metabolite perturbation heatmaps (Supplementary Figure S2B).

The combination treatment resulted in a more substantial disruption of the metabolome, with 418 (403 decreased and 15 increased), 274 (270 decreased and 4 increased) and 366 (360 decreased and 6 increased) metabolites significantly perturbed at 1, 3 and 6 h, respectively (Supplementary Figure S3). Polymyxin B monotherapy induced a slightly lower global metabolite perturbation, affecting 354 metabolites (350 decreased and 4 increased) at 1 h, 241 metabolites (231 decreased and 10 increased) at 3 h, and only 270 metabolites (266 decreased and 4 increased) at 6 h (Supplementary Figure S3). In contrast, Leu_{10}-teixobactin monotherapy exhibited a less pronounced effect, displaying a time-dependent perturbation pattern. At 1 h, only 9 metabolites (4 decreased and 5 increased) were perturbed, while at 3 h, 10 metabolites were affected, all of which decreased. However, the most substantial effect occurred at 6 h, wherein Leu_{10}-teixobactin perturbed a larger number of metabolites, with a total of 75 (72 decreased and 3 increased) significantly affected metabolites (Supplementary Figure S3).

The metabolic profiling analysis of the significantly altered metabolites indicated that the combination treatment (across all-time points) largely perturbed (mainly decreased) peptides, amino acids and carbohydrates. There was a minor impact on nucleotides, lipids, cofactors and vitamins (Supplementary Figure S4A). Likewise, albeit to a lesser degree, polymyxin B monotherapy induced a similar pattern of alterations, with the most notable changes observed in peptides, amino acids, and carbohydrates (Supplementary Figure S4A). Conversely,

Leu_{10}-teixobactin monotherapy predominantly suppressed the levels of carbohydrates, peptides and nucleotides intermediates, particularly evident at 6 h (Supplementary Figure S4A). Interestingly, Venn diagrams showed that the combination treatment induced unique significant metabolites at each time point, with 76, 49, and 82 unique metabolites affected at 1, 3, and 6 h, respectively (Supplementary Figure S4B). There was a gradual increase in the number of commonly affected intermediates across all treatment conditions, 3 (1 h), 9 (3) and 50 (6 h) (Supplementary Figure S4B). Intriguingly, at 6 h, the combination treatment shared approximately 70% of its intermediates with polymyxin B and around 20% with Leu_{10}-teixobactin monotherapies (Supplementary Figure S4B). In the following discussions we provide a specific network level break-down of the key metabolite classes impacted by the combination treatment.

Global lipid metabolism

Fatty acids and glycerophospholipids are fundamental components of Gram-negative bacterial membranes, providing structural integrity, regulating membrane fluidity, and serving as a selective barrier for molecule transport across the membrane[27]. At 1 h, the combination therapy exhibited a pronounced perturbation across all lipid classes, including fatty acids and glycerophospholipids, compared to the polymyxin B and Leu_{10}-teixobactin monotherapies. However, this impact diminished at later time points, 3 and 6 h (Fig. 2).

Fatty acids

At 1 h, the combination treatment impacted the abundance of nine essential fatty acids (FA), among which were hydroxylated fatty acids FA hydroxy(16:0) (log_2FC=-2.6) and FA hydroxy(18:1) (log_2FC=-3.3). These fatty acids are integral components of bacterial membrane, and playing a crucial in maintaining its structural integrity and function. They play diverse roles in modifying bacterial cell envelope properties, affecting permeability to various molecules, including antibiotics and antimicrobial peptides[28–31]. It was observed that polymyxin B monotherapy also reduced the abundance of six fatty acids intermediates, albeit to a lesser extent. These include oleoyl-CoA, trans-hexadec-2-enoyl-CoA, FA oxo(14:0), FA (14:1), FA hydroxy(16:0) and FA trihydroxy(18:1) ($log_2FC \geq$ -1.0, p-value < 0.05; Fig. 2). At later time points (3 h and 6 h), the impact of both the combination and polymyxin B monotherapy on fatty acids intermediates declined, with fewer fatty acids affected (Fig. 2). Notably, Leu_{10}-teixobactin treatment had a minimal effect on fatty acid levels, perturbing only one fatty acid intermediate [FA (16:2), log_2FC=-2.8] at 6 h (Fig. 2).

Phospholipids

The combination treatment induced extensive perturbations of ten essential glycerophospholipids at 1 h (Fig. 2). Notably, among these phospholipids were cytidine diphosphate-diacylglycerol (CDP-DG; log_2FC=-5.5), *sn*-glycerol 3-phosphate (log_2FC=-3.0), and *sn*-glycero-3-phosphoethanolamine (log_2FC= -3.4). At the same time point, polymyxin B monotherapy induced perturbations in a smaller number of lipids compared to the combination treatment, with lower intensity of perturbation observed for shared phospholipids (e.g., *sn*-glycero-3-phosphoethanolamine, log_2FC=-2.9 and *sn*-glycerol 3-phosphate, log_2FC=-2.0; Fig. 2). Conversely, Leu_{10}-teixobactin monotherapy had minimal effect on phospholipid intermediates, with only two intermediates, namely PA(32:2) and PI(20:1), exhibiting decreased levels ($log_2FC \geq$ -1.0, p-value < 0.05; Fig. 2).

The inhibitory effect of the combination on essential phospholipids (e.g., *sn*-glycerol 3-phosphate, log_2FC_{3h} =-1.8 and log_2FC_{6h}=-1.2; CDP-DG, log_2FC_{3h} =-1.5 and log_2FC_{6h}=-1.9) persisted at later time points (3 and 6 h), while the impact of polymyxin B monotherapy significantly diminished (Fig. 2). Leu_{10}-teixobactin monotherapy showed increased perturbation at 6 h, with five lipid precursors (e.g., 2-C-Methyl-D-erythritol 4-phosphate, log_2FC=-1.3 and CDP-DG (16:0/18:2[9Z,12Z])), log_2FC=-1.4), decreased in abundance (Fig. 2).

These perturbed phospholipids are critical for maintaining the structural integrity, fluidity, and functionality of the bacterial membrane[32]. CDP-DG is involved in various cellular signaling pathways[33]. Importantly, *sn*-glycero-3-phosphoethanolamine and *sn*-glycerol 3-phosphate are integral to the structure and function of the bacterial cell envelope in Gram-negative bacteria. Specifically, they play roles in lipid bilayers formation, LPS transport, membrane fluidity, cell division, and serves as key intermediates for the biosynthesis phospholipids[34,35]. A recent study has shown that increased *sn*-glycerol 3-phosphate levels in *Pseudomonas aeruginosa* could hinder growth, lower pyocyanin synthesis, impair motility, reduce tolerance to oxidative stress and increased resistance to kanamycin[36].

Cell envelope biogenesis

The cell wall structure of Gram-negative bacteria comprises an inner membrane consisting of a phospholipid bilayer and FAs, a thin peptidoglycan layer, and an outer membrane composed of phospholipids and LPS[37]. Amino- and nucleotide-sugars are crucial for peptidoglycan and LPS biosynthesis[38,39].

The combination treatment inhibited key amino- and nucleotide-sugar intermediates, such as UDP-*N*-acetylglucosamine (UDP-GlcNAc) and UDP-*N*-acetylmuramate (UDP-MurNAc), across all time points (1, 3 and 6 h; $log_2FC \geq$ -1.0, p-value < 0.05; Fig. 3). Notably, these precursors are assembled on the lipid carrier undecaprenol phosphate during peptidoglycan synthesis to form key cell wall intermediates, lipid I and lipid II, which are specifically targeted by teixobactin[15,40]. The combination treatment also decreased the abundance of five essential downstream components in the peptidoglycan biosynthesis pathway.

These components include UDP-*N*-acetylmuramoyl-L-alanyl-D-gamma-glutamyl-*meso*-2,6 diaminopimelate (UDP-MurNAc-L-Ala-y-D-Glu-*m*-DAP), UDP-*N*-acetylmuramoyl-L-alanyl-D-glutamyl-6-carboxy-L-lysyl-D-alanyl-D-alanine [UDP-MurNAc-L-Ala-y-D-Glu-*m*-DAP-D-Ala(2)], UDP-N-acetylmuramoyl-L-alanyl-D-glutamyl-*meso*-2,6-diaminoheptanedioate-D-alanine (UDP-MurNAc-L-Ala-y-D-Glu-m-DAP-D-Ala), D-alanyl-D-alanine and D-alanine ($log_2FC \geq$ -1.0, p-value < 0.05 ; Fig. 3). Further, the combination treatment led to a significant decrease in essential precursors required for LPS formation across all time points. These

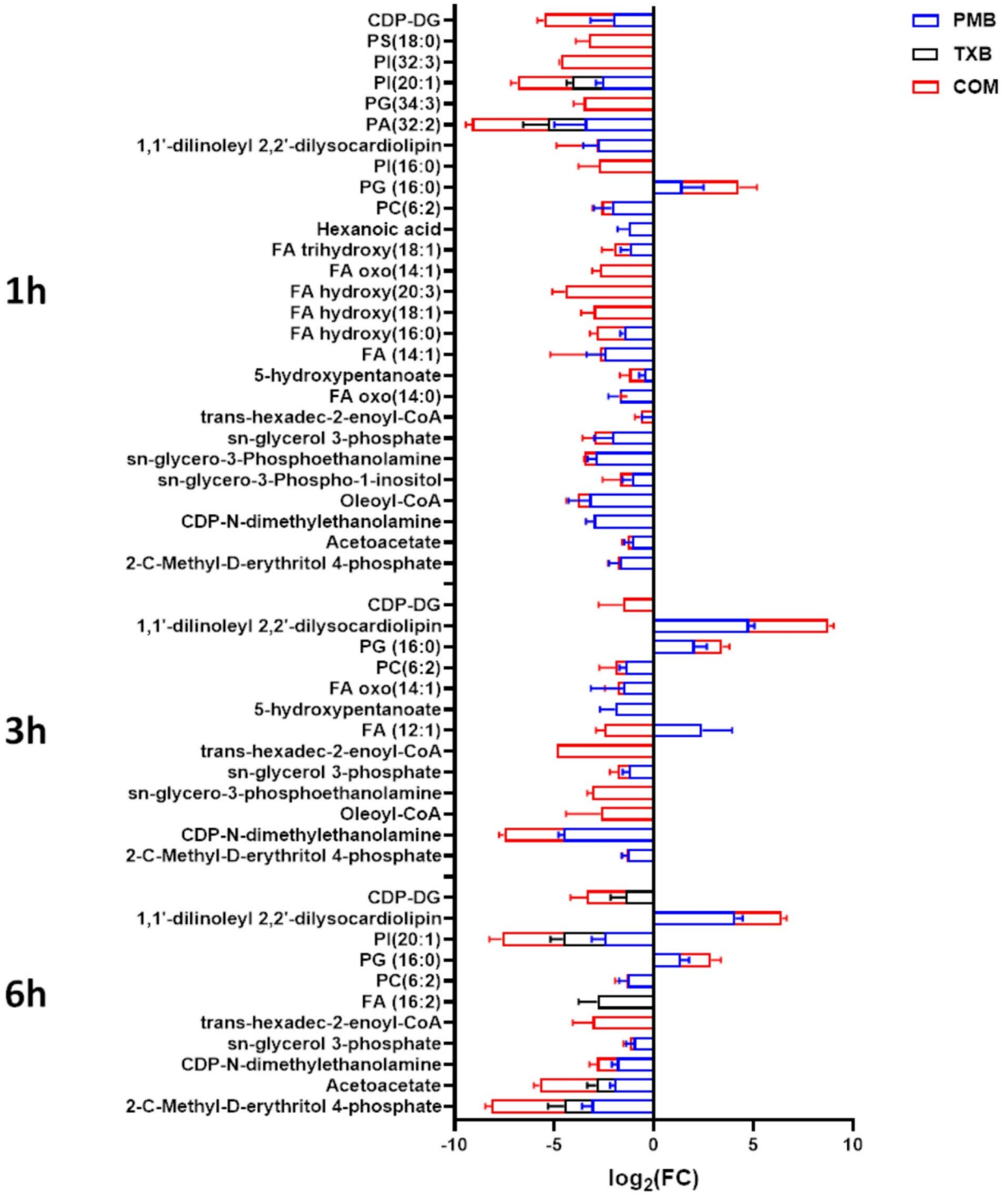

Fig. 2. Significantly perturbed lipids at 1, 3 and 6 h in*A. baumannii*ATCC™ 19606 following treatment with polymyxin B (PMB, Blue), Leu_{10}-teixobactin (TXB, Black) monotherapies and their combination (Com, Red). Lipid names are putatively assigned based on accurate mass (log_2-fold change (FC) ≥ 0.58 or ≤ -0.58, corresponding to a metabolite level change of approximately 1.5-fold; FDR-adjusted p-value < 0.05). PG, glycerophosphoglycerols; glycerophosphoglycerols; PS, glycerophosphoserines; PC, glycerophosphocholines; PA, glycerophosphates; PI; FA, fatty acids; CDP-DAG, Cytidine diphosphate diacylglycerol.

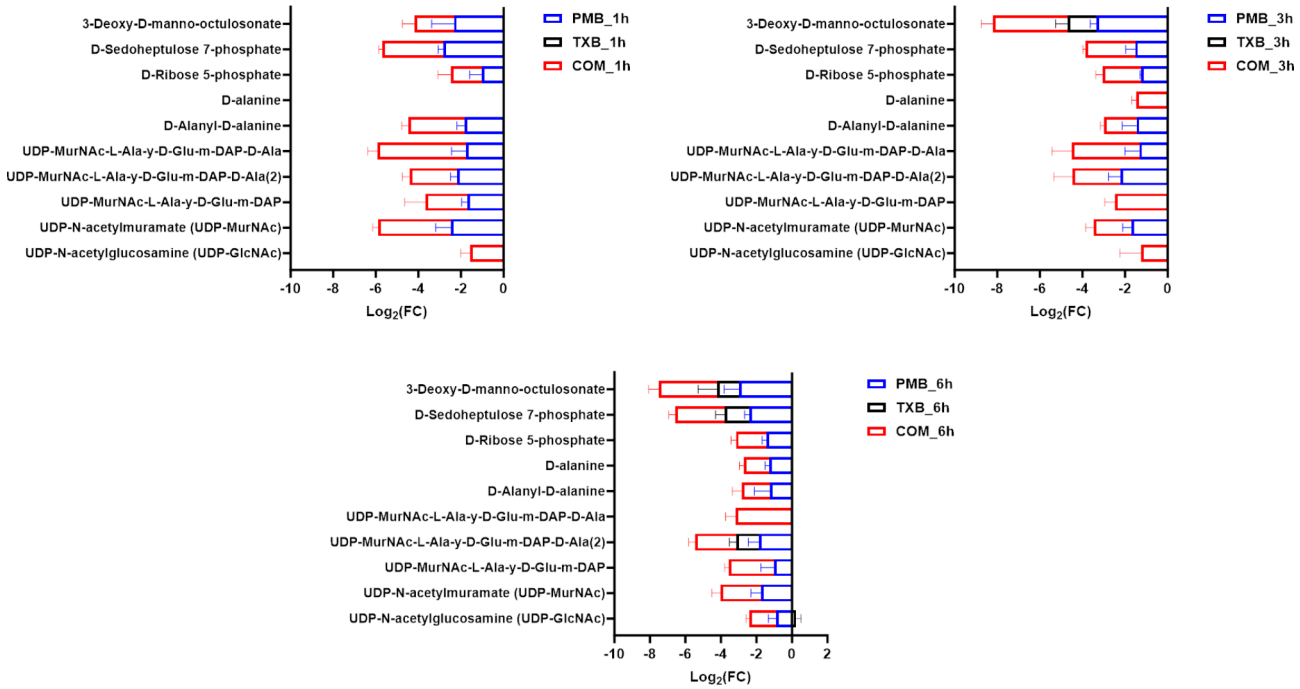

Fig. 3. Impact of polymyxin B, Leu_{10}-teixobactin monotherapies and their combination on bacterial cell envelope biogenesis. The bar charts illustrate the significantly impacted metabolites after 1, 3, and 6 h exposure. Perturbed metabolites were primarily involved in amino-sugar and nucleotide-sugar metabolism and downstream pathways, peptidoglycan and lipopolysaccharide (LPS) biosynthesis in *A. baumannii* ATCC™ 19606 in response to treatment with polymyxin B (PMB, blue) or Leu_{10}-teixobactin (TXB, black) monotherapy and their combination (COM, red). Log_2-fold change (FC) ≥ 0.58 or ≤ -0.58, corresponding to a metabolite level change of approximately 1.5-fold; FDR-adjusted p-value < 0.05.

precursors included D-sedoheptulose 7-phosphate and D-ribulose 5-phosphate and 3-deoxy-D-manno-octulosonate (KDO) ($log_2FC \geq -1.0$, p-value < 0.05; Fig. 3). D-sedoheptulose 7-phosphate serves as a heptose unit crucial for the core structure of LPS in Gram-negative bacteria, and also acts as a central metabolite within the pentose phosphate pathway[41,42].

Although polymyxin B monotherapy perturbed the same metabolic pathways (i.e., amino- and nucleotide-sugar metabolism, peptidoglycan and LPS biogenesis), the extent of disruption was comparatively less pronounced both in terms of the number of affected metabolites and the magnitude of the perturbation in metabolite levels when compared to the combination treatment across all time points ($log_2FC \geq -0.58$, p-value < 0.05; Fig. 3). Leu_{10}-teixobactin monotherapy demonstrated even milder effects on the aforementioned pathways, including the primary precursor UDP-GlcNAc involved in lipid I and II synthesis. Nevertheless, it is noteworthy to mention that Leu_{10}-teixobactin monotherapy markedly reduced the abundance of KDO at 3 h (log_2FC=-1.3) and 6 h (log_2FC=-1.2; Fig. 3).

Cellular respiration

The combination treatment caused a dramatic decrease in the levels of key intermediates regulating the tricarboxylic acid (TCA) cycle. This effect was most pronounced at 6 h and was less pronounced at the earlier time points of 1 and 3 h. Among the significantly impacted precursors were citrate, fumarate, succinate, malate 2-oxoglutarateand acetyl-CoA ($log_2FC \geq -1.0$, p-value < 0.05; Fig. 4).

Interestingly, it has been reported that reduced levels of fumarate and succinate significantly increased the susceptibility of stationary-phase *P. aeruginosa* to the aminoglycoside antibiotic tobramycin[43,44]. Intermediates of the electron transport chain (ETC), also underwent significant perturbations in response to the combination treatment, with the most pronounced impact observed at 3 and 6 h (Fig. 4). This was evident by a marked decline in the levels of ATP, ADP, NAD, orthophosphate, and pyrophosphate ($log_2FC \geq -1.0$, p-value < 0.05; Fig. 4). This effect is likely drive by polymyxin B which we have previously reported acts as a potent inhibitor of the ETC enzyme NADH-quinone oxidoreductase in Gram-negative bacteria[45].

Polymyxin B monotherapy perturbed the TCA cycle (e.g., citrate and succinate) and ETC elements (e.g., NAD) across all time points 1, 3 and 6 h ($log_2FC \geq -1.0$, p-value < 0.05; Fig. 4). By comparison to the combination treatment, the impact of polymyxin B monotherapy on the TCA cycle and ETC metabolites was moderate in terms of both the number of affected metabolites and the extent of perturbation in metabolite levels across all time points. In line with the well documented delayed antibacterial activity of Leu_{10}-teixobactin against Gram-positive bacteria[15], Leu_{10}-teixobactin monotherapy perturbed five key elements of the TCA cycle (e.g., acetyl-

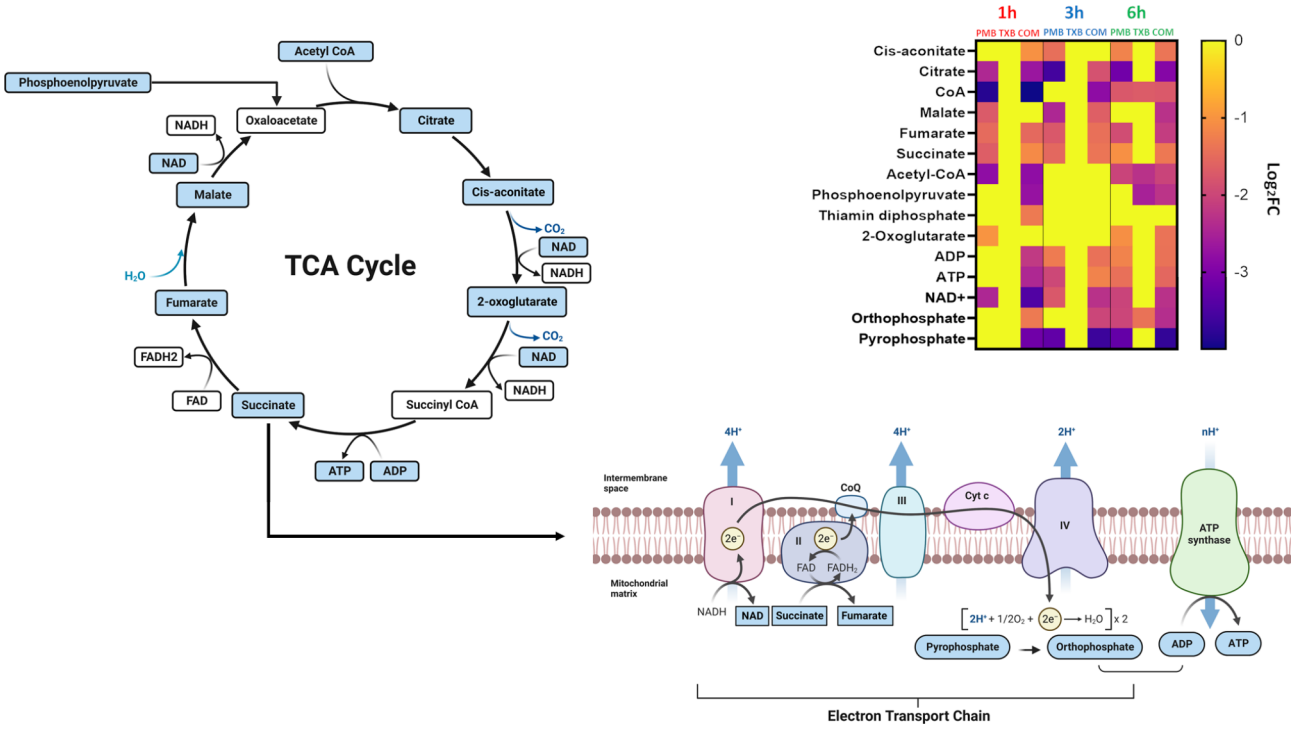

Fig. 4. Impact of polymyxin B, Leu_{10}-teixobactin monotherapies and their combination on bacterial cellular respiration. Schematic diagram and heatmap depicting the significantly impacted metabolites involved in cellular respiration pathways at 1, 3, and 6 h post exposure, namely the tricarboxylic acid (TCA) cycle and electron transport chain pathways, of *A. baumannii* ATCC™ 19606. The alterations are shown following treatment with polymyxin B (PMB, blue) or Leu_{10}-teixobactin (TXB, black) monotherapies and their combination (COM, red) (log_2-fold change (FC) ≥ 0.58 or ≤ -0.58, corresponding to a metabolite level change of approximately 1.5-fold; FDR-adjusted p-value < 0.05). Blue rectangles: significantly inhibited metabolites; Red rectangles: Significantly increased metabolites. The figure was partly created with BioRender.com.

CoA, log_2FC=-2.2; phosphoenolpyruvate, log_2FC=-2.5) and one component of the ETC (orthophosphate, log_2FC=-1.4) after the extended exposure period of 6 h (Fig. 4).

Peptidoglycan assay

To determine the effects of polymyxin B and Leu_{10}-teixobactin, alone and in combination, on the peptidoglycan biosynthetic pathway, we compared the total peptidoglycan abundance between untreated and treated *A. baumannii* ATCC™19606 cultures. No significant differences were observed at 1 and 3 h; however, at 6 h, peptidoglycan levels were significantly decreased following combination treatment compared to monotherapies and the untreated control (Fig. 5).

These findings confirm that the combination of polymyxin B and Leu_{10}-teixobactin disrupts peptidoglycan production in *A. baumannii* ATCC™ 19606. The decrease in peptidoglycan abundance at 6 h aligns with the observed metabolic disruptions and the time-dependent perturbation profile in our metabolomics results.

The results support the well-known mechanism of teixobactin impacting peptidoglycan biosynthesis[15,19,23]. Additionally, previous studies have shown that polymyxins also disrupt peptidoglycan biosynthesis[4,39,46]. This perturbation likely contributes to the synergistic effect observed with the polymyxin B and Leu_{10}-teixobactin combination against *A. baumannii*.

Scanning electron microscopy and transmission electron microscopy

Scanning electron microscopy (SEM) and transmission electron microscopy (TEM) were employed to investigate the impact of polymyxin B (2 mg/L) and Leu_{10}-teixobactin (4 mg/L) monotherapy and their combination, on the cellular morphology and membrane structures of *A. baumannii* ATCC™ 19606 at 1 h exposure (Fig. 6).

SEM images revealed blebbing, protrusions, and morphological changes in bacterial cells treated with polymyxin B monotherapy, whereas the cells treated with Leu_{10}-teixobactin alone, displayed some dehydration, albeit showing minimal morphological changes. Combination therapy induced extensive damage to the bacterial cell membrane, resulting in significant blebbing, protrusions, vacuole formation, and perforation to the cell envelope, indicating that the antibiotic combination effectively induced extensive damage to membrane structures.

TEM analysis complemented all of the above SEM observations by unveiling further detailed ultrastructural changes (Fig. 6). Polymyxin B monotherapy caused membrane damage, characterized by blebbing and irregularities in the cell envelope. Leu_{10}-teixobactin monotherapy mediated minimal intracellular vesicle

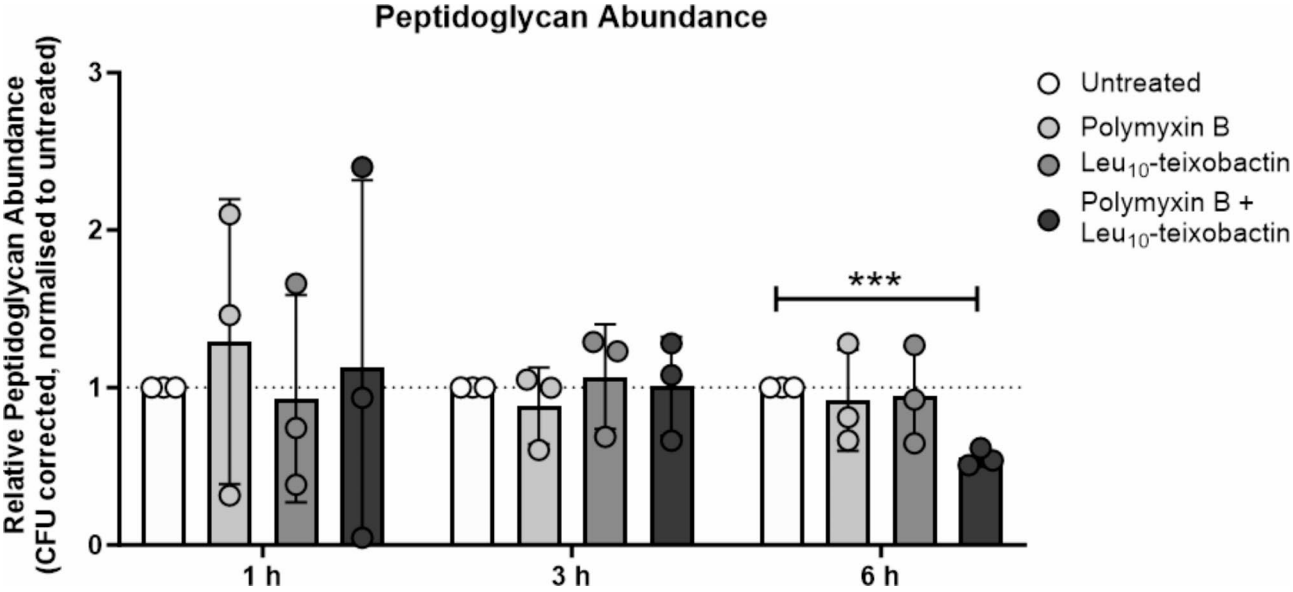

Fig. 5. Impact of polymyxin B, Leu_{10}-teixobactin monotherapies and their combination on bacterial peptidoglycan abundance. Detection of peptidoglycan from cultures of *A. baumannii* ATCC™ 19606 grown either untreated or treated with polymyxin B (1 μg/mL), Leu_{10}-teixobactin (4 μg/mL), or polymyxin B (1 μg/mL) + Leu_{10}-teixobactin (4 μg/mL) in combination, at 1 h, 3 h, and 6 h post-treatment. Data represent the mean ± standard deviation of three independent biological experiments. Statistical significance was determined by an unpaired *t*-test, *** = $p < 0.001$.

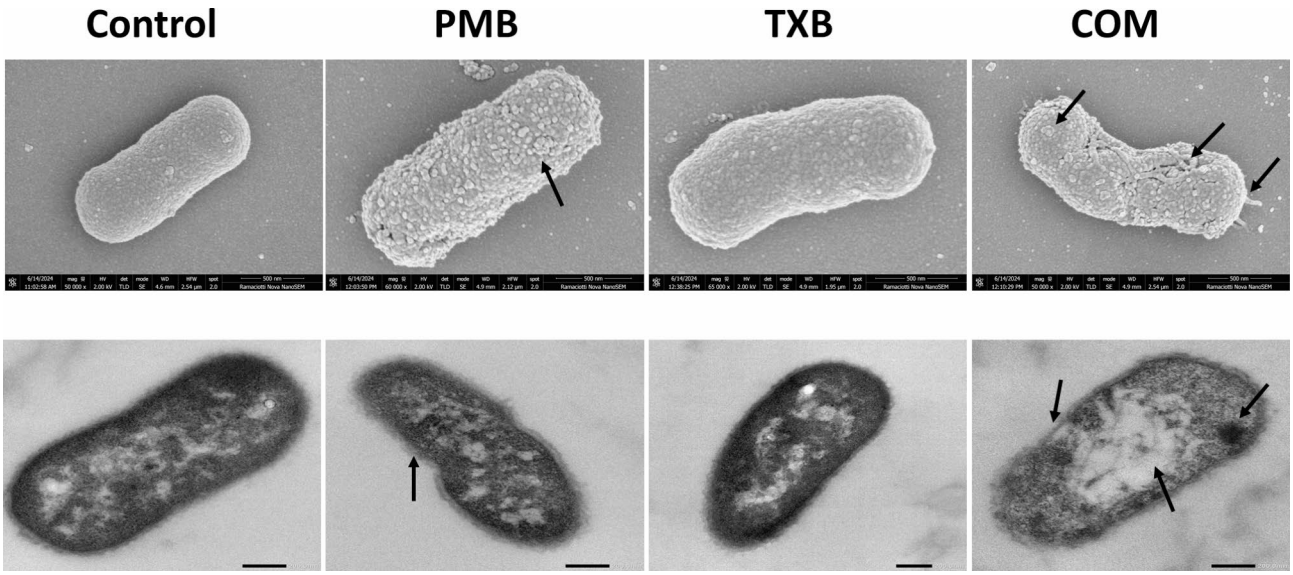

Fig. 6. Electron microscopy images. Scanning electron microscopy (Scale 500 nm) and transmission electron microscopy (Scale 200 nm) images of *A. baumannii* ATCC™ 19606, 1 h after treatment with polymyxin B (PMB, 2 μg/mL), Leu_{10}-teixobactin (TXB, 4 μg/mL), or polymyxin B (2 μg/mL) + Leu_{10}-teixobactin (4 μg/mL) in combination (COM).

formation. The combination therapy led to an apparent increase in membrane disruption and cellular damage, including chromatin condensation, and vesicle and vacuole formation. By comparison to the monotherapies, the combination treatment indicates a substantially greater impact on bacterial membranes.

Conclusions

This study is first to investigate the synergistic antibacterial activity of polymyxin B in combination with Leu_{10}-teixobactin against both polymyxin-susceptible and -resistant *A. baumannii* strains. Analysis of the *A. baumannii* ATCC™19606 metabolome revealed that multiple interrelated metabolic pathways played a crucial role in the

synergistic killing activity of the combination. The disrupted pathways were primarily those responsible for maintaining the integrity of the bacterial cell envelope, particularly the biosynthesis of LPS and peptidoglycan. The combination treatment significantly inhibited essential precursors (e.g., UDP-GlcNAc and UDP-MurNAc) of early peptidoglycan biosynthesis and lipid I and lipid II formation. Significant perturbations in cellular respiration pathways (e.g., TCA cycle and electron transport chain) were also observed (Fig. 7).

Peptidoglycan detection assays showed a significant decrease in peptidoglycan levels at 6 h following combination treatment, confirming disrupted peptidoglycan production. Electron microscopy provided further insights, with SEM and TEM images showing extensive damage to the bacterial cell membrane and morphology as a result of the combination therapy, compared to monotherapies and untreated cells.

These findings suggest that the initial outer membrane permeabilizing action of polymyxin B facilitates the entry of Leu_{10}-teixobactin into the Gram-negative bacterial cells, enabling it to reach its lipid I/II intracellular targets. and as such allows the 'resistance-resistant' action of teixobactin to impede the regrowth of resistant sub-populations or mutants (Fig. 1)[15,47].

Overall, the study underscores the promising potential of the polymyxin B-Leu_{10}-teixobactin combination as an effective treatment against MDR *A. baumannii* infections and offers valuable insights into bacterial killing synergy, paving the way for developing innovative, mechanism-based targeted therapies.

Materials and methods

Chemicals and reagents

The teixobactin analogue, Leu_{10}-teixobactin, was synthesized in our lab as detailed later below[19]. Polymyxin B (Beta Pharma, China) stock solution was dissolved in Milli-Q water (Millipore, Australia) and sterilised by 0.22-µm syringe filters (Sartorius, Australia). Cation-adjusted Mueller-Hinton (CAMHB) broth media (Oxoid, England) were prepared from Mueller-Hinton broth (MHB) adjusted with 22.5 mg/L $CaCl_2$ and 11.25 mg/L $MgCl_2$.

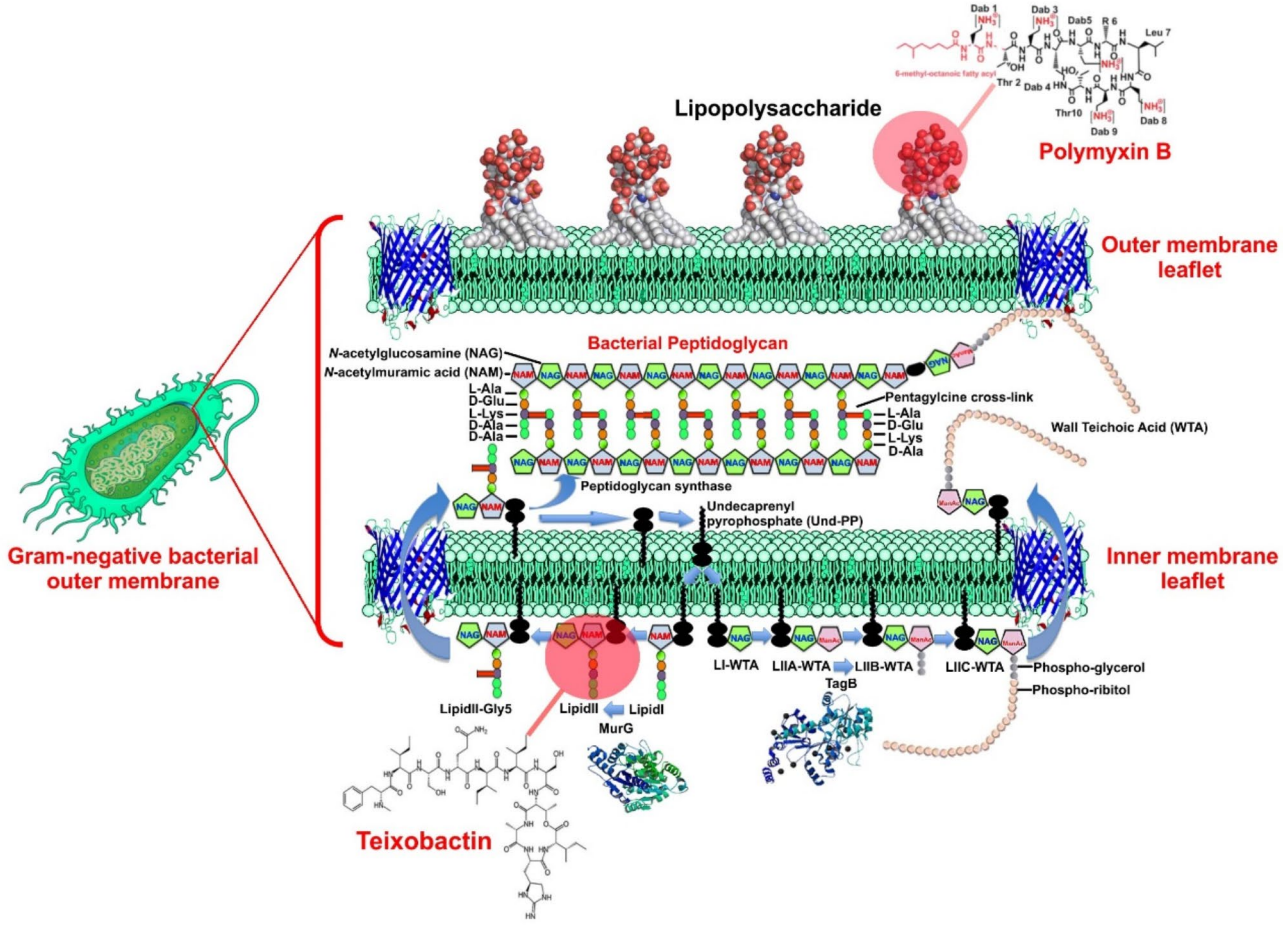

Fig. 7. Schematic diagram. Summarizing the key metabolic perturbations in *A. baumannii* ATCC™ 19606 in response to polymyxin B and Leu_{10}-teixobactin combination treatment. The figure was created with BioRender.com.

Bacterial isolates

Twelve different *A. baumannii* isolates, including four polymyxin B-susceptible (ATCC^{TM}19606, ATCC^{TM}17978, FADDI-AB150, FADDI-AB151) and eight polymyxin B-resistant strains (FADDI-AB143, FADDI-AB144, FADDI-AB145, FADDI-AB146, FADDI-AB148, FADDI-AB149, FADDI-AB060, FADDI-AB065), were employed in this study.

Determination of minimum inhibitory concentration (MIC) and fractional inhibitory concentration (FIC)

The minimum inhibitor concentration (MIC) is defined as the lowest concentration of antimicrobial agent that shows a complete inhibition of visible bacterial growth after overnight incubation. The susceptibility breakpoints for polymyxin B were defined as susceptible ($\leq$2 mg/L) and resistant ($\geq$4 mg/L) according to the clinical & laboratory standards institute (CLSI) guidelines[48]. The MICs of polymyxin B and Leu_{10}-teixobactin were determined for all bacterial isolates in triplicate on separate days using broth microdilution checkerboard assays according to CLSI guidelines and are documented in Supplementary Table S1. Polymyxin B and Leu_{10}-teixobactin stock solutions were prepared immediately before each experiment. Polymyxin B powder was dissolved in MilliQ water and sterilized by membrane syringe filters with a pore size of 0.22 micron (ThermoFisher Scientific, Melbourne, VIC, Australia). Leu_{10}-teixobactin was dissolved in dimethyl sulfoxide (DMSO; Sigma-Aldrich, Melbourne, VIC, Australia). Serial concentrations of DMSO (0.12, 0.25%, 0.5%, 1%, 2.5% v/v) showed no inhibitory effect against all bacteria tested. Serial dilutions (2-fold) of the polymyxin B and Leu_{10}-teixobactin were prepared in a cation-adjusted Mueller–Hinton broth (CAMHB; Oxoid, Basingstoke, UK) supplemented with 0.1% Tween 80 to prevent adhesion of Leu_{10}-teixobactin to the 96-well microtiter plates for obtaining solutions with various concentrations[19,23]. To ensure that Tween 80 did not exhibit any antibacterial effect, a vehicle control of 0.1% Tween 80 alone was tested in the 96-well plates and showed no antibacterial effect. The experiments were performed in 96-well microtiter plates (Techno Plas, Adelaide, SA, Australia) in broth culture containing ~ 10^6 CFU/mL of the bacteria. The microdilution plates were incubated at 37 °C for 18–20 h.

The synergy tests for the combination were conducted using the fractional inhibitory concentration index (FICI) analysis. The formula used to calculate the FIC values was as follows: FICI = (MIC of drug A in combination ÷ MIC of drug A alone) + (MIC of drug B in combination ÷ MIC of drug B alone). The FICI results were defined as: synergism FIC < 0.5; addition FIC = 0.5–1.0; indifference FIC = 1–4; antagonism FIC $\geq$ 4[44]. An MIC of 128 µg/mL for teixobactin was used to calculate the FICI scores.

Static time-kill assays

Static time-kill assays were performed to investigate the antibacterial killing kinetics of polymyxin B, Leu_{10}-teixobactin, and their combination[49]. Overnight cultures of each *A. baumannii* strain were prepared by inoculating one colony into 10 mL of CAMHB in a 50 mL falcon tube (Thermo Fisher Scientific, Australia) and incubating in a shaking water bath (150 rpm) at 37 °C for 16 h. Next, bacterial cultures were diluted to the early log phase (OD600 ~ 0.5) by inoculating into fresh CAMHB and incubating for 2 h. The bacterial suspensions were then transferred to 50 mL glass Erlenmeyer flask (Pyrex, Australia), and stock solutions of the antibiotics were added to achieve final concentrations of polymyxin B (0.5 mg/L), Leu_{10}-teixobactin (4 mg/L), and the combination (polymyxin B [0.5 mg/L] plus Leu_{10}-teixobactin [4 mg/L]). Following drug treatment, flasks of bacterial suspensions were incubated at 37 °C and shaking speed of 150 rpm. Control groups were treated with equivalent volume of solvents as the antibiotic treatments and incubated at the same conditions. Each treatment was performed in triplicate. After 24 h incubation at 37 °C, viable cell counting (colony forming units per millilitre [CFU/mL]) was performed using an automated spiral plater (Don Whitley Scientific, Australia).

Time-kill curves were generated by plotting $\log_{10}$ (CFU/mL) against time (h). Significant bacterial killing activity was defined as a $\geq$3 $\log_{10}$ decrease in CFU/mL compared with the untreated control samples. Antimicrobial synergy of the antibiotic combination was defined as a reduction of $\geq$2 $\log_{10}$CFU/mL compared to the most active single agent of the combination[49].

Bacterial culture preparation for metabolomics

Time-kill assays were conducted in triplicate during the late exponential phase (~ 10^8 CFU/mL) to evaluate the pharmacodynamic activity of polymyxin B, Leu_{10}-teixobactin, and their combination, and to optimize the experimental conditions (Supplementary Figure S5). Overnight bacterial cultures of *A. baumannii* ATCC™ 19606 were prepared by inoculating a single colony into 10 mL of CAMHB in a 50 mL Falcon tube and incubating at 37 °C in a water bath shaker set to 150 rpm for 16 h. The following day, a 100-fold dilution of the overnight culture was prepared by transferring a small amount into 500 mL conical flasks (×4) containing fresh CAMHB. These flasks were immediately incubated in an incubator shaker (Bioline) at 37 °C with shaking at 180 rpm until reaching the log phase, indicated by an optical density at 600 nm (OD_{600}) of approximately 0.5, corresponding to a cell density of ~ 10^8 CFU/mL.

Stock solutions of polymyxin B, Leu_{10}-teixobactin or their combination were added accordingly to three treatment flasks, with final concentrations of 1 mg/L for polymyxin B, 4 mg/L for Leu_{10}-teixobactin, and the respective combination concentrations; the fourth flask served as the untreated control. Samples of 15 mL were collected at each time point (1, 3 and 6 h) and immediately quenched to stop further bacterial metabolism. Subsequently, all samples were normalized with fresh CAMHB to obtain pre-treatment OD_{600} values. Bacterial cells were pelleted by centrifugation at 3220 × *g* at 4 °C for 10 min, and the supernatants were removed subsequently. The pellets were then stored at -80 °C, awaiting metabolite extraction. Each treatment condition was performed in quadruplicate to reduce the bias from inherent random variation.

Metabolite extraction

The pellets were washed by 0.9% NaCl and centrifuged at 3220 × *g* at 4˚C for 5 min to remove the residual medium (x2). The washed pellets were then resuspended in a cold extraction solvent (chloroform/methanol/water 1:3:1; v/v/v) containing 1 µM of each internal standard (CHAPS, CAPS, PIPES and TRIS). To release intracellular metabolites, the samples were subjected to freeze-thaw cycles, alternating between immersion in liquid nitrogen and thawing on ice, followed by vortexing. Subsequently, samples were transferred to 1.5 mL Eppendorf tubes and centrifuged at 14,000 × *g* at 4˚C for 10 min. Finally, 200 µL of the resulting supernatants were aliquoted to injection vials for LC-MS analysis. A pooled biological quality control (PBQC) sample was prepared by combining an equal volume of each extracted sample for LC-MS analysis.

LC-MS analysis

The LC-MS analysis was conducted following our previously established protocol[31]. Samples were injected into a nano-high-performance liquid chromatography (nano-HPLC) system (Dionex UltiMate 3000 RSLCnano System; Thermo Fisher Scientific), equipped with a ZIC-pHILIC column (SeQuant, 5 µm, polymeric, 150 × 4.6 mm; Merck), and coupled to a Q-Exactive Orbitrap mass spectrometer (Thermo Fisher Scientific, Australia). The mass spectrometer operated in positive/negative ion–switching electron-spray ionisation (ESI) mode, with a full scan range set at 85–1275 m/z and a resolution of 35,000. The column temperature was maintained at 25˚C. Metabolites were eluted using a mobile phase consisting of 20 mM ammonium carbonate (A) and acetonitrile (B) in different ratios, following a multi-step gradient manner. Solvent B started at 80% and was gradually reduced to 50% over 15 min, then further decreased to 5% over 18 min. Subsequently, the column was washed with 5% solvent B for 3 min and re-equilibrated with 80% solvent B at a flow rate of 0.3 mL/min over 8 min for the next batch. All sample and PBQC samples were randomized and analyzed throughout the analysis. Prior to LC-MS analysis, blank samples containing mixtures of authentic standards were analyzed for quality control purposes[50].

LC-MS data processing and metabolite annotation

The raw LC-MS data underwent processing and metabolite annotation using the IDEOM workflow, following established methods[50]. Initially, the raw data were converted to mzXML files. Subsequently, LC-MS peak signals were extracted utilizing the Centwave algorithm within XCMS[51]. The samples were aligned, and artifacts were filtered out using mzMatch[52]. Additional noise filtering and feature identification were conducted based on accurate mass and retention time[53].

A retention time prediction model was developed using multiple linear regression, trained on the retention times of authentic standards from the LC-MS analysis. This model was further refined through mass recalibration[54]. The retention time of metabolites recorded in databases retrieved from KEGG, Biocyc/Metacyc, LIPIDMAPS, and HDMB was then predicted automatically using the retention time prediction model. Filtered features were given a confidence score for metabolite identification based on accurate mass (± 2 ppm), retention time error (± 50%) (observed retention time versus calculated retention time) and match to database of interest. For this study, an organism-specific database curated for *A. baumannii* ATCC^{TM}19606, based on functional annotations of the genome, was utilized[55].

Statistical analysis

The raw peak intensity generated in CSV files were uploaded into MetaboAnalyst 5.0 [56]. Putative metabolites with a median RSD ≤ 0.2 (20%) within the QC group and IDEOM confidence level ≥ 5 were incorporated into a table and then uploaded to MetaboAnalyst[57]. Half of the minimum positive values in the original data were used to replace features with > 25% missing values. The interquartile range was used to filter the data followed by $\log_2$ transformation and auto scaling to normalize the data. One-way ANOVA ($p < 0.05$ for Fisher's LSD; fold change threshold = 1.5) was used to identify metabolites with significant changes between control and treatment groups. KEGG mapper was used to build the metabolic pathway modules by uploading the KEGG IDs of the statistically significant metabolites[58].

Synthesis of Leu10-teixobactin

Synthesis was undertaken using 2-Chlorotrityl Chloride Resin (0.1 mmol) (100–200 mesh 0.4-1.0 mmol/g). The first amino acid (Leu_{10}) was loaded using a 6 molar equivalents solution of Fmoc-amino acid [Fmoc = 9-fluorenylmethoxycarbonyl] in *N*, *N*-dimethylformamide (DMF). The rest of the amino acids from 1 to 10 were coupled via the Protein Technologies Prelude automated peptide synthesizer using standard Fmoc solid-phase peptide chemistry. Coupling of the Fmoc-amino acids was performed using the default instrument protocol: 3 molar equivalents (relative to resin loading) of the Fmoc amino acid and HCTU [1-[Bis(dimethylamino)methylene]-1 H-1,2,3-triazolo[4,5-b] pyridinium 3-oxid hexafluorophosphate] in DMF with activation in situ, using 6 molar equivalents of *N*, *N*-diisopropylethylamine (DIPEA). This was carried out for 50 min at room temperature. Fmoc deprotection was conducted using the default instrument protocol: 20% piperidine in DMF (1 × 5 min, 1 × 10 min) at room temperature. The synthesized peptide (1–10) resin was dried overnight. In another flask, the Fmoc-Ile-OH (5 equivalent) was dissolved in dry DMF under nitrogen, then 5 equivalent DIC was added dropwise at 0 °C, and the mixture was stirred for 5 min. After the activation of Fmoc-Ile-OH acid, the overnight dried resin was transferred into the solution, 0.3 equivalent 4-dimethylaminopyridine (DMAP) was added, and the reaction mixture was stirred overnight.

The synthesized linear peptide resin was utilized before the deprotection of the Ile11 Fmoc protecting group by 20% piperidine for 5 min twice. The protected linear peptide was then cleaved from the resin by treating the resin with 20% hexafluoroisopropanol (HFIP) in dichloromethane (DCM) (1 × 30 min, 1 × 5 min). This solution was concentrated under a vacuum to give the crude-protected linear peptide. The protected linear peptide was dissolved in DMF (5 mL) to which DIPEA 0.6 mmol, 104 µL (6 molar equivalents relative to the loading of the

resin) and diphenylphosphoryl azide (DPPA), 0.3 mmol, 0.65 µL (3 molar equivalents relative to the loading of the resin) were added. The solution was shaken overnight at room temperature. The reaction solution was then concentrated under a vacuum for a minimum of 6 h to give the crude-protected cyclic peptide. The resulting residue was taken up in a solution of 2.5% 3,6-dioxa-1,8-octanedithiol (DODT) and 5% triisopropylsilane (TIPS) in trifluoroacetic acid (TFA) and stirred at room temperature for 90 min. To this solution, 40 mL of diethyl ether was added. The precipitate was centrifuged and washed twice with diethyl ether (40 mL), then air-dried in a fume hood to give the crude cyclic peptide (a pale-yellow solid). The resulting solid was taken up in Milli-Q water (5 mL) and de-salted using a Vari-Pure IPE SAX column. The crude cyclic lipopeptide was then subjected to RP-HPLC. Leu_{10}-teixobactin (Supplementary Figure S6A) was obtained in a yield of 7.4 mg, retention time (Rt) at 214 nm = 15.23 min (purity: 94.5%). ESI-MS analysis of peak at 15.23 min: m/z (monoisotopic) [M + 1 H]1 + 1202.10 [M + 2 H]2 + 601.85. Calculated mass (monoisotopic) for teixobactin (C58H96N12O15) 1201.71 (Supplementary Figure S6B).

Peptidoglycan detection assay

Detection of peptidoglycan was conducted using a muramic acid quantitation protocol modified from[59]. Briefly, *A. baumannii* ATCC™ 19606 was cultured on LB agar overnight and a single colony was inoculated into 10 mL of cation-adjusted Mueller-Hinton broth (CAMHB) in a 50 mL Falcon tube and incubated at 37 °C, shaking at 180 rpm overnight. The following day, the culture was diluted 1:100 in fresh CAMHB (20 mL) and incubated for approximately 3 h at 37 °C in an Innova shaking incubator (180 rpm) to reach OD_{600} 0.5. Cultures were either left untreated, or treated with polymyxin B (1 µg/mL), Leu_{10}-teixobactin (4 µg/mL), or polymyxin B (1 µg/mL) + Leu_{10}-teixobactin (4 µg/mL) in combination. At 1, 3 and 6 h post-treatment, 1 mL of the cultures were withdrawn and normalized to OD_{600} 0.5 prior to harvesting via centrifugation at 18,000 ×*g* for 5 min.

Cells were washed once in 1 mL sterile PBS with 20 µL taken for CFU enumeration. The cell pellets were resuspended in 100 µL 1 M NaOH and left to incubate at 38°C for 30 min, prior to addition of 100 µL 0.5 M H_2SO_4 and 1 mL concentrated H_2SO_4 (~ 18 M). Samples were incubated at 96°C for 7 min and cooled on ice prior to addition of 10 µL 4% [w/v] $CuSO_4$ and 20 µL 1.5% [w/v] 4-phenylphenol in 96% ethanol with immediate mixing. Samples were then incubated for a further 30 min at 30°C before determination of OD_{560} in a clear, 96 well plate using a CLARIOStar spectrophotometer (BMG Labtech). Colony forming units were enumerated after overnight growth on LB agar plates at 37°C and OD_{560} was corrected for CFU/mL for each culture and normalized to untreated. Statistical analyses were performed in GraphPad Prism version 10.0.1.

Scanning and transmission electron microscopy

Scanning and transmission electron microscopy were performed as we have previously described[60].

Data availability

The entirety of our raw data is available at MetaboLights under the study identifier MTBLS10862. Any additional data can be obtained from the corresponding author on reasonable request.

Received: 2 August 2024; Accepted: 4 November 2024
Published online: 07 November 2024

References

1. Dadgostar, P. Antimicrobial resistance: Implications and costs. *Infect. Drug Resist.* **12**, 3903–3910 (2019).
2. Russo, A. et al. Bloodstream infections caused by carbapenem-resistant *Acinetobacter baumannii*: Clinical features, therapy and outcome from a multicenter study. *J. Infect.* **79** (2), 130–138 (2019).
3. Ventola, C. L. The antibiotic resistance crisis: Part 1: Causes and threats. *P t.* **40** (4), 277–283 (2015).
4. Hussein, M. et al. Mechanisms underlying synergistic killing of polymyxin B in combination with cannabidiol against *Acinetobacter baumannii*: A metabolomic study. *Pharmaceutics* **14** (4) (2022).
5. Tacconelli, E. *Global Priority List of Antibiotic-Resistant Bacteria to Guide Research, Discovery, and Development*. (2017).
6. Organization, W. H. & WHO Bacterial Priority Pathogens List. *Bacterial Pathogens of Public Health Importance to Guide Research, Development and Strategies to Prevent and Control Antimicrobial Resistance 2024*. 72. (2024).
7. Mulani, M. S., Kamble, E. E., Kumkar, S. N., Tawre, M. S. & Pardesi, K. R. Emerging strategies to combat ESKAPE pathogens in the era of antimicrobial resistance: A review. *Front. Microbiol.* **10**, 539 (2019).
8. Abadi, A., Rizvanov, A., Haertlé, T. & Blatt, N. World health organization report: Current crisis of antibiotic resistance. *BioNanoScience*. **9**, 778–788 (2019).
9. Velkov, T. et al. Teaching 'old'polymyxins new tricks: new-generation lipopeptides targeting gram-negative 'superbugs'. *ACS Chem. Biol.* **9** (5), 1172–1177 (2014).
10. Landman, D., Georgescu, C., Martin, D. A. & Quale, J. Polymyxins revisited. *Clin. Microbiol. Rev.* **21** (3), 449–465 (2008).
11. Li, Z., Cao, Y., Yi, L., Liu, J. H. & Yang, Q. Emergent polymyxin resistance: End of an era? *Open. Forum Infect. Dis.* **6** (10) (2019).
12. Cheah, S. E. et al. Polymyxin resistance in *Acinetobacter baumannii*: Genetic mutations and transcriptomic changes in response to clinically relevant dosage regimens. *Sci. Rep.* **6** (1), 26233 (2016).
13. Bergen, P. J. et al. Rational combinations of polymyxins with other antibiotics. In *Polymyxin Antibiotics: From Laboratory Bench to Bedside*. 251–288. (Springer, 2019).
14. Trimble, M. J., Mlynárčik, P., Kolář, M. & Hancock, R. E. Polymyxin: Alternative mechanisms of action and resistance. *Cold Spring Harbor Perspect. Med.* **6** (10), a025288 (2016).
15. Ling, L. L. et al. A new antibiotic kills pathogens without detectable resistance. *Nature*. **517** (7535), 455–459 (2015).
16. Parmar, A. et al. Teixobactin analogues reveal enduracididine to be non-essential for highly potent antibacterial activity and lipid II binding. *Chem. Sci.* **8** (12), 8183–8192 (2017).
17. Karas, J. A. et al. Synthesis and structure – activity relationships of teixobactin. *Ann. N. Y. Acad. Sci.* **1459** (1), 86–105 (2020).
18. Giltrap, A. M. et al. Total synthesis of teixobactin. *Org. Lett.* **18** (11), 2788–2791 (2016).
19. Hussein, M. et al. The killing mechanism of teixobactin against methicillin-resistant *Staphylococcus aureus*: An untargeted metabolomics study. *mSystems* **5** (3) (2020).

20. Velkov, T. et al. The impact of backbone N-methylation on the structure-activity relationship of Leu10-teixobactin. *J. Pept. Sci.* **25** (9), e3206 (2019).
21. Parmar, A. et al. Design and syntheses of highly potent teixobactin analogues against *Staphylococcus aureus*, Methicillin-Resistant *Staphylococcus aureus* (MRSA), and vancomycin-resistant enterococci (VRE) *in Vitro* and *in vivo*. *J. Med. Chem.* **61** (5), 2009–2017 (2018).
22. Shukla, R. et al. Teixobactin kills bacteria by a two-pronged attack on the cell envelope. *Nature*. **608** (7922), 390–396 (2022).
23. Homma, T. et al. Dual targeting of cell wall precursors by teixobactin leads to cell lysis. *Antimicrob. Agents Chemother.* **60** (11), 6510–6517 (2016).
24. Ng, V., Kuehne, S. A. & Chan, W. C. Rational design and synthesis of modified teixobactin analogues: In vitro antibacterial activity against *Staphylococcus aureus*, propionibacterium acnes and *Pseudomonas aeruginosa*. *Chemistry (Weinheim Der Bergstrasse Germany)*. **24** (36), 9136–9147 (2018).
25. Li, J. et al. Antibiograms of multidrug-resistant clinical *Acinetobacter baumannii*: Promising therapeutic options for treatment of infection with colistin-resistant strains. *Clin. Infect. Dis.* **45** (5), 594–598 (2007).
26. Belley, A. et al. Assessment by time-kill methodology of the synergistic effects of oritavancin in combination with other antimicrobial agents against *Staphylococcus aureus*. *Antimicrob. Agents Chemother.* **52** (10), 3820–3822 (2008).
27. Rowlett, V. W. et al. Impact of membrane phospholipid alterations in *Escherichia coli* on cellular function and bacterial stress adaptation. *J. Bacteriol.* **199** (13), 00849-16.
28. de Carvalho, C. & Caramujo, M. J. The various roles of fatty acids. *Molecules* **23** (10). (2018).
29. Nikaido, H., Hancock, R. & Sokatch, J. Outer membrane permeability of *Pseudomonas aeruginosa*. *Bacteria*. **10**, 145–193 (2012).
30. Mansilla, M. C., Cybulski, L. E., Albanesi, D. & de Mendoza, D. Control of membrane lipid fluidity by molecular thermosensors. *J. Bacteriol.* **186** (20), 6681–6688 (2004).
31. Hussein, M. et al. Metabolomics study of the synergistic killing of polymyxin B in combination with amikacin against polymyxin-susceptible and-resistant *Pseudomonas aeruginosa*. *Antimicrob. Agents Chemother.* **64** (1), e01587–e01519 (2019).
32. Kurita, K., Kato, F. & Shiomi, D. Alteration of membrane fluidity or phospholipid composition perturbs rotation of MreB complexes in *Escherichia coli*. *Front. Mol. Biosci.* **7**, 364 (2020).
33. Jennings, W. & Epand, R. M. CDP-diacylglycerol, a critical intermediate in lipid metabolism. *Chem. Phys. Lipids*. **230**, 104914 (2020).
34. Zhang, Y. M. & Rock, C. O. Membrane lipid homeostasis in bacteria. *Nat. Rev. Microbiol.* **6** (3), 222–233 (2008).
35. Cronan, J. E. Jr & Vagelos, P. R. Metabolism and function of the membrane phospholipids of *Escherichia coli*. *Biochim. Biophys. Acta (BBA)-Rev. Biomembr.* **265** (1), 25–60 (1972).
36. Liu, Y. et al. Metabolic mechanism and physiological role of glycerol 3-phosphate in Pseudomonas aeruginosa PAO1. *mBio*. **13** (6), e0262422 (2022).
37. Silhavy, T. J., Kahne, D. & Walker, S. The bacterial cell envelope. *Cold Spring Harb Perspect. Biol.* **2** (5), a000414 (2010).
38. Plumbridge, J. & Vimr, E. Convergent pathways for utilization of the amino sugars N-acetylglucosamine, N-acetylmannosamine, and N-acetylneuraminic acid by *Escherichia coli*. *J. Bacteriol.* **181** (1), 47–54 (1999).
39. Hussein, M. et al. Mechanistic insights from global metabolomics studies into synergistic bactericidal effect of a polymyxin B combination with tamoxifen against cystic fibrosis MDR *Pseudomonas aeruginosa*. *Comput. Struct. Biotechnol. J.* **16**, 587–599 (2018).
40. van Heijenoort, J. Lipid intermediates in the biosynthesis of bacterial peptidoglycan. *Microbiol. Mol. Biol. Rev.* **71** (4), 620–635 (2007).
41. Taylor, P. L. et al. Structure and function of sedoheptulose-7-phosphate isomerase, a critical enzyme for lipopolysaccharide biosynthesis and a target for antibiotic adjuvants. *J. Biol. Chem.* **283** (5), 2835–2845 (2008).
42. Hussein, M. et al. Unique mechanistic insights into pathways associated with the synergistic activity of polymyxin B and caspofungin against multidrug-resistant *Klebsiella pneumoniae*. *Comput. Struct. Biotechnol. J.* **20**, 1077–1087 (2022).
43. Liu, Y., Yang, K., Zhang, H., Jia, Y. & Wang, Z. Combating antibiotic tolerance through activating bacterial metabolism. *Front. Microbiol.* **11**, 577564 (2020).
44. Meylan, S. et al. Carbon sources tune antibiotic susceptibility in *Pseudomonas aeruginosa* via tricarboxylic acid cycle control. *Cell. Chem. Biol.* **24** (2), 195–206 (2017).
45. Deris, Z. Z. et al. A secondary mode of action of polymyxins against Gram-negative bacteria involves the inhibition of NADH-quinone oxidoreductase activity. *J. Antibiot.* **67** (2), 147–151 (2014).
46. Maifiah, M. H. M. et al. Untargeted metabolomics analysis reveals key pathways responsible for the synergistic killing of colistin and doripenem combination against *Acinetobacter baumannii*. *Sci. Rep.* **7** (1), 45527 (2017).
47. Ejim, L. et al. Combinations of antibiotics and nonantibiotic drugs enhance antimicrobial efficacy. *Nat. Chem. Biol.* **7** (6), 348–350 (2011).
48. CLSI. *The Clinical & Laboratory Standards Institute (CLSI) Guidelines* (CLSI, 2020).
49. Barry, A. L. et al. Methods for determining bactericidal activity of antimicrobial agents; Approved guideline. *NCCLS Document M26-A. Clinical and Laboratory Standards Institute, Wayne, PA [Google Scholar]* (1999).
50. Srivastava, A. & Creek, D. J. Using the IDEOM workflow for LCMS-based metabolomics studies of drug mechanisms. *Methods Mol. Biol.* **2104**, 419–445 (2020).
51. Tautenhahn, R., Böttcher, C. & Neumann, S. Highly sensitive feature detection for high resolution LC/MS. *BMC Bioinform.* **9** (1), 504 (2008).
52. Scheltema, R. A., Jankevics, A., Jansen, R. C., Swertz, M. A. & Breitling, R. PeakML/mzMatch: A file format, Java library, R library, and tool-chain for mass spectrometry data analysis. *Anal. Chem.* **83** (7), 2786–2793 (2011).
53. Creek, D. J., Jankevics, A., Burgess, K. E. V., Breitling, R. & Barrett, M. P. IDEOM: An excel interface for analysis of LC–MS-based metabolomics data. *Bioinformatics*. **28** (7), 1048–1049 (2012).
54. Creek, D. J. et al. Toward global metabolomics analysis with hydrophilic interaction liquid chromatography–mass spectrometry: Improved metabolite identification by retention time prediction. *Anal. Chem.* **83** (22), 8703–8710 (2011).
55. Zhu, Y. et al. Metabolic responses to polymyxin treatment in *Acinetobacter baumannii* ATCC 19606: Integrating transcriptomics and metabolomics with genome-scale metabolic modeling. *mSystems* **4**(1). (2019).
56. Chong, J., Wishart, D. S. & Xia, J. Using MetaboAnalyst 4.0 for comprehensive and integrative metabolomics data analysis. *Curr. Protoc. Bioinf.* **68** (1), e86 (2019).
57. Pang, Z. et al. Using MetaboAnalyst 5.0 for LC–HRMS spectra processing, multi-omics integration and covariate adjustment of global metabolomics data. *Nat. Protoc.* **17** (8), 1735–1761 (2022).
58. Kanehisa, M. & Sato, Y. KEGG Mapper for inferring cellular functions from protein sequences. *Protein Sci.* **29** (1), 28–35 (2020).
59. Hadžija, O. A simple method for the quantitative determination of muramic acid. *Anal. Biochem.* **60** (2), 512–517 (1974).
60. Abdul Rahim, N. et al. Synergistic killing of NDM-producing MDR *Klebsiella pneumoniae* by two 'old'antibiotics—Polymyxin B and chloramphenicol. *J. Antimicrob. Chemother.* **70** (9), 2589–2597 (2015).

Acknowledgements

J. L. is an Australian National Health and Medical Research Council (NHMRC) Principal Research Fellow, and T. V. is an Australian Research Council Mid-Career Industry Fellow. The authors acknowledge the assistance

provided by the Ramaciotti Centre for Cryo-Electron Microscopy, Monash University, the Victorian Node of Microscopy Australia.

Author contributions

Conceptualization, M.H.; Data curation, M.H., Z.K., S.N. and R.A.; Formal analysis, M.H.; Funding acquisition, J.L.,T.V. and G.R.; Investigation, M.H., R.A. and Z.K.; Methodology, M.H., S.N., V.T., A.K.; Resources, M.B., J.W., M.B., C.M, S.C.; Software, M.H., M.M., A.K.; Supervision, J.L., T.V.; Validation, G.R., J.L. and T.V.; Writing – original draft, M.H.; Writing – review & editing, M.H., S.N., C.M., M.B., R.G., J.L. and T.V.

Funding

G.R., T.V., an J.L. are supported by the National Institute of Allergy and Infectious Diseases, award numbers R01AI146241, R01AI170889. The content is solely the responsibility of the authors and does not necessarily represent the official views of the National Institutes of Health.

Declarations

Competing interests

The authors declare no competing interests.

Additional information

Supplementary Information The online version contains supplementary material available at https://doi.org/10.1038/s41598-024-78769-6.

Correspondence and requests for materials should be addressed to M.H., G.G.R., J.L. or T.V.

Reprints and permissions information is available at www.nature.com/reprints.

Publisher's note Springer Nature remains neutral with regard to jurisdictional claims in published maps and institutional affiliations.